INTERGRANULAR CREEP FRACTURE IN NIMONIC 80A UNDER CONDITIONS OF CONSTANT CAVITY DENSITY

B. F. Dyson and M. J. Rodgers*

INTRODUCTION

Experimental creep fracture studies have identified three sequential but overlapping stages to intergranular creep fracture: (1) nucleation of individual cavities on grain boundary facets, (2) their growth and subsequent interlinkage to form single grain facet cracks and (3) the formation of multiple grain facet cracks of sufficient length to enable a single dominant crack to grow and cause failure. In principle, each stage can control fracture lifetime but most theoretical models concerned with predicting time to fracture have assumed that stages 1 and 3 are sufficiently rapid for stage 2 to become rate controlling. These theories [1 - 5] assume that cavity growth is due to stress directed diffusion of vacancies from perfect sources at grain boundaries to perfect sinks at the cavity surface. In all cases, the resulting expression for fracture lifetime (t_f) has the form:

$$t_f = \frac{Z\, s^3}{D_B\, \sigma_1} \tag{1}$$

where D_B is the grain boundary diffusivity, s is the cavity spacing and σ_1 is the maximum principal applied stress. Z is a structure insensitive parameter whose value depends on the boundary conditions assumed in solving the vacancy flux equation, as well as on the detailed formulation of the fracture criterion.

Although doubt has been expressed frequently on the relevance of equation (1) to creep fracture, the equation has never been subjected to an unambiguous test because of the difficuly of ensuring that a prescribed number of cavity nuclei are present at some known instant in time, preferably at the start of the creep test. The limited objective of the present paper is to assess the applicability of equation (1) to Nimonic 80A by making use of a novel way of introducing intergranular cavities into this material [6].

EXPERIMENTAL PROCEDURE

A quantifiable density of intergranular cavities can be introduced into Nimonic 80A simply by plastically deforming it at room temperature and then heating for a suitable time at an elevated temperature. The number density and size of these cavities are independent of the stress state imposed during deformation (for example, compression or tension [7]) but are strongly dependent on the subsequent thermal history after plastic

*Division of Materials Applications, National Physical Laboratory, Teddington, England.

deformation [6, 8]. Thus all specimens were given a standard heat treatment of 2h at 750°C prior to creep. This treatment ensured that the initial cavity spacing s was a unique one, independent of both the applied creep stress and the temperature of testing, since the constant-load uniaxial creep tests were performed subsequently at temperatures $\leq$ 750°C. Figure 1 is an electron micrograph, taken with an AEI 1 MeV electron microscope, illustrating the size, spacing and approximately spherical shape of these cavities before application of the creep load. The mean spacing was 0.75 μm and the mean initial diameter 0.21 μm.

RESULTS AND DISCUSSION

Four uniaxial creep tests were performed at stresses ranging from 150 to 460 MPa at a constant temperature of 750°C and five tests were performed at a stress of 460 MPa in the temperature range 575°C to 750°C. All fractures were intergranular with elongation less than 4%. Figure 2 illustrates the typical cavity distribution, size and spacing seen by optical microscopy in a longitudinal section of a fractured specimen about 10 mm from the fracture face.

The average cavity spacing after creep fracture is 1.5 μm and the shape is still approximately circular in two dimensions although there are some elliptically shaped cavities with their major axis along the trace of the grain boundary. Figure 2 clearly illustrates the preference of cavities for transverse boundaries.

The fracture lifetimes for the varying stress/temperature are shown in Figures 3 and 4. These results can be expressed in the form:

$$t_f = H\,\sigma^{-n} \exp\left(\frac{Q}{kT}\right) \qquad (2)$$

where H is a constant, n = 4 and Q = 337 kJ mole^{-1}.

Equation (1), in contrast, predicts that n = 1 and Q = 180 kJ mole^{-1} (taking the mean grain boundary activation energy for nickel measured by Cannon and Stark [9] as representative of Nimonic 80A).

To calculate whether equation (1) under-estimates or over-estimates the experimental rupture lifetimes requires a knowledge of the absolute values of Z, s and D_B, all of which are subject to either modelling or experimental errors. Nevertheless, an upper bound to fracture lifetimes predicted by equation (1) can be found by taking maximum values of Z and s and minimum values for D_B. Comparison of the various theoretical models [1 - 5] shows that the maximum value of Z is given by the approximate one of the two expressions given by Hull and Rimmer [1] viz:

$$Z = \frac{kT}{4\Omega\delta} \qquad (3)$$

where δ is the grain boundary width, Ω is the atomic volume and kT has its usual meaning.

Since s at fracture was found to differ by a factor of 2 from that at the start of creep, the larger value of 1.5 μm is used. Cannon and Stark's

[9] data for nickel provides a lower bound value for D_B of 10^{-14} m^2 s^{-1}. Curve (b) in Figure 3 was derived using these values of Z, s and D_B and curve (b) in Figure 4 was constructed using, in addition, an activation energy of 180 kJ mole^{-1}. Figures 3 and 4 show clearly that the stress-directed diffusive cavity growth theories of creep fracture under-estimate the creep rupture resistance of Nimonic 80A even when an upper bound is calculated - the lower bound prediction to lifetime is approximately three orders of magnitude lower. The values of n and Q are more akin to those found for the stress exponent and activation energy for creep deformation and in fact the limited data in Figures 3 and 4 can be represented by an equation of the form:

$$t_f = \frac{1}{(\dot{\varepsilon}_m)^{0.93}} \qquad (3)$$

where $\dot{\varepsilon}_m$ is the minimum creep rate.

It would appear therefore that deformation rate is strongly influencing creep fracture resistance even in this special case when all the cavities are present at the start of creep. Two possible explanations present themselves in the light of our present understanding of creep fracture outlined in the introduction. Firstly, the criterion of fracture which is assumed may be in error so that stage 3 becomes the rate controlling process. Evidence has been presented in other alloys in support of stage 3 control (for example Venkiteswaran and Taplin [10]), but it remains an unquantified stage. It is likely to be strongly dependent on the magnitude of the ratio $\sigma_1/\bar{\sigma}$, where $\bar{\sigma}$ is the von Mises effective stress and thus lifetime will be a function of stress state. A second possible explanation is that the cavity growth is less than that predicted by stress directed diffusion of vacancies and is controlled by the grain deformation rate. If this explanation were true, creep fracture would be independent of stress state except near the limit of $\sigma_1 \to 0$.

CONCLUSIONS AND FUTURE WORK

Uniaxial creep experiments have shown that lifetime in Nimonic 80A is given by equation (2), with n = 4 and Q = 337 kJ mole^{-1}. The material was treated prior to creep in order to introduce a known density of cavities so that a comparison could be made with the diffusive growth theories of creep fracture. There was no agreement between theory and experiment and the theory grossly under-estimated creep fracture resistance. Future work will aim at establishing the cause of this discrepancy between theory and experiment. Cavity growth rate measurements will be made to determine whether stage 2 is rate-controlling, by virtue of a reduced cavity growth rate, and creep experiments under a different state of stress will be performed to study the importance of stage 3.

REFERENCES

1. HULL, D. and RIMMER, D. E., Phil. Mag. 4, 1959, 673.
2. SPEIGHT, M. V. and HARRIS, J. E., Met. Sci. J. 1, 1967, 83.
3. VITOVEC, F. H., J. Mat. Sci. 7, 1972, 615.
4. WEERTMAN, J., Met. Trans. 5, 1974, 1743.
5. RAJ, R. and ASHBY, M. F., Acta. Met. 23, 1975, 653.

6. DYSON, B. F. and HENN, D. E., J. of Microscopy 97, 1973, 165.
7. DYSON, B. F., LOVEDAY, M. S. and RODGERS, M. J., Proc. Roy. Soc. A349, 1976, 245.
8. DYSON, B. F. and LOVEDAY, M. S., work to be published.
9. CANNON, R. F. and STARK, J. P., J.A.P. 40, 1969, 4366.
10. VENKITESWARAN, P. K. and TAPLIN, D. M. R., Met. Sci. 8, 1974, 97.

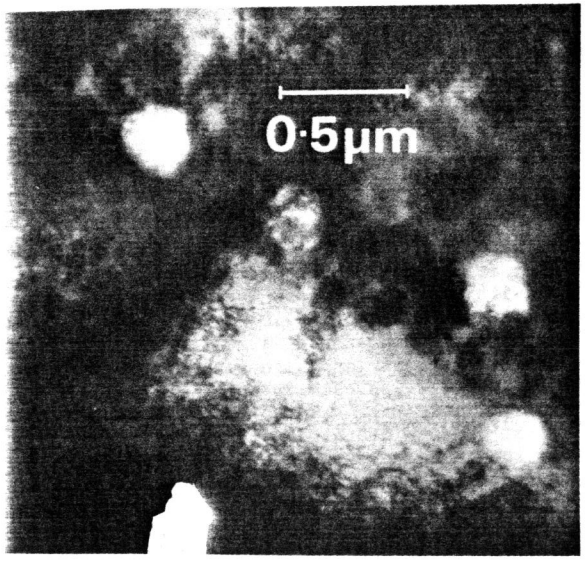

Figure 1 1MeV Electron Micrograph Illustrating the Size and Spacing of Cavities at the Start of Creep

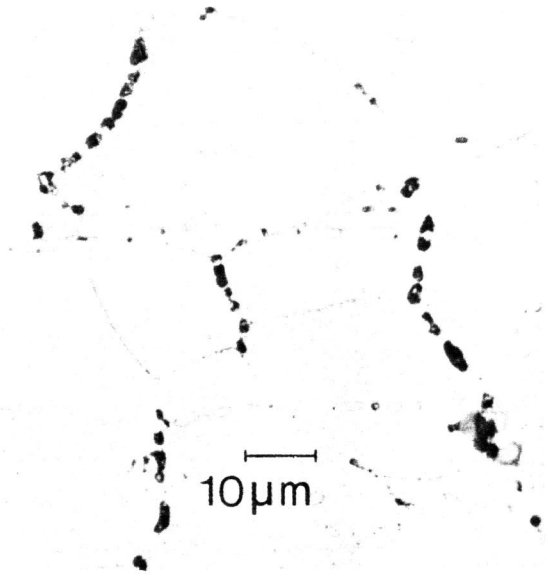

Figure 2 Optical Micrograph Illustrating the Distribution, Size and Spacing of Cavities near to Creep Fracture Face. The Creep Stress Axis is Horizontal

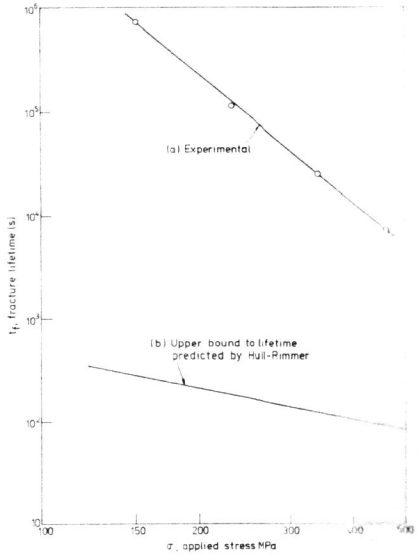

Figure 3 (a) Experimental Values of Time to Fracture versus Applied Stress at 750° C

(b) The Computed Upper Bound to Fracture as a Function of Stress Predicted by Hull and Rimmer

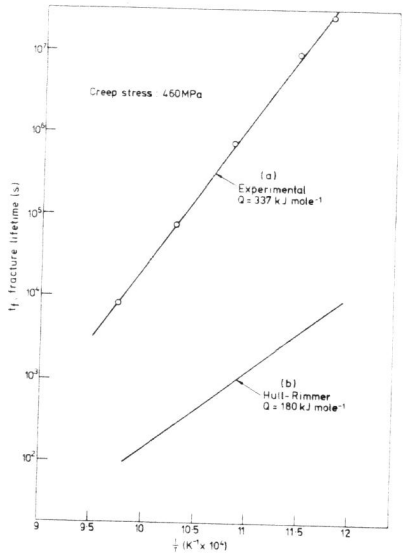

Figure 4 (a) Experimental Data of Time to Fracture versus Reciprocal of the Absolute Temperature for a Stress of 460 MPa

(b) The Computed Upper Bound to Fracture as a Function of Temperature Predicted by Hull and Rimmer